

# Bi-objective facility location in the presence of uncertainty

Najmesadat Nazemi <sup>a</sup>, Sophie N. Parragh <sup>a</sup>, Walter J. Gutjahr <sup>b</sup>

<sup>a</sup> Institute of Production and Logistics Management, Johannes Kepler University Linz  
Altenberger Strae 69, 4040 Linz, Austria  
[{najmesadat.nazemi, sophie.parragh}@jku.at](mailto:{najmesadat.nazemi, sophie.parragh}@jku.at)

<sup>b</sup> Department of Statistics and Operations Research, University of Vienna  
Oskar-Morgenstern-Platz 1, 1090 Vienna, Austria  
[walter.gutjahr@univie.ac.at](mailto:walter.gutjahr@univie.ac.at)

## Abstract

Multiple and usually conflicting objectives subject to data uncertainty are main features in many real-world problems. Consequently, in practice, decision-makers need to understand the trade-off between the objectives, considering different levels of uncertainty in order to choose a suitable solution. In this paper, we consider a two-stage bi-objective location-allocation model to design a last-mile network in disaster relief where one of the objectives is subject to demand uncertainty. We analyze scenario-based two-stage risk-neutral stochastic programming, adaptive (two-stage) robust optimization, and a two-stage risk-averse stochastic approach using conditional value-at-risk (CVaR). To cope with the bi-objective nature of the problem, we embed these concepts into two criterion space search frameworks, the  $\epsilon$ -constraint method and the balanced box method, to determine the Pareto frontier. We propose a decomposition-based algorithm to deal with the computationally challenging representation of the two-stage CVaR model. Additionally, a matheuristic technique is developed to obtain high-quality approximations of the Pareto frontier for large-size instances. Finally, we evaluate and compare the performance of the applied approaches based on real-world data from a Thies drought case, Senegal.

**Keywords:** Multi-objective optimization, Uncertainty, Facility location problem, Humanitarian relief

# 1 Introduction

Decision-makers (DMs) often face multiple goals, which are in conflict with each other (Ehrgott, 2005), e.g., minimization of cost vs. maximization of service level, and, finding a feasible solution that simultaneously optimizes all criteria is usually impossible. Consequently, it is important for DMs to understand the trade-off between the considered objectives. To cope with this issue, many real-world problems have been modeled as multi-objective optimization (MOO) problems and, a variety of algorithms have been developed to produce the set of trade-off solutions.

Moreover, usually, DMs do not make their decisions in a completely certain environment. Depending on the problem, different levels of uncertainty should be taken into account to make reliable decisions. To deal with this issue in optimization problems, different approaches have been proposed in the literature. The most widely used ones are stochastic programming (Birge and Louveaux, 2011) and robust optimization (Ben-Tal et al., 2009). Stochastic optimization assumes that the underlying probability distributions of the uncertain parameters are known or can be estimated, e.g., based on historical data. It allows to model different risk attitudes, e.g., risk-neutral decision making (the expected value) or risk-averse decision making (risk measure). Unlike stochastic optimization, robust optimization does not assume any probabilistic data but only uncertain parameters stemming from an uncertainty set (e.g., scenarios). Well-known robust concepts are minmax/static robustness and adaptive robust optimization (Bertsimas et al., 2011).

Although many different approaches have been developed to cope with multiple objectives and uncertainty separately in optimization problems, the intersection of these two main domains, i.e., the analysis of decision problems involving multiple objectives and parameter uncertainty simultaneously, only received comparably little attention. Combinations of MOO with stochastic programming concepts (Abdelaziz, 2012; Gutjahr and Pichler, 2016) and robustness concepts (Ehrgott et al., 2014; Ide and Schöbel, 2016) give a flavor of the diverse possible ways to cope with real-life decision making problems.

Optimization problems arising along the humanitarian relief chain (HRC) are real-world applications that motivated us in combining bi-objective optimization and optimization under uncertainty, as multiple objectives and inherent risk are distinguishing features of humanitarian logistics. HRC problems concern multi-stakeholder decision making in which a population of stakeholders seeks to balance their conflicting objectives and priorities. The objectives can be categorized into three main groups of criteria, efficiency criteria, effectiveness criteria, and equity criteria (Gralla et al., 2014). Besides, in a disaster situation, most of the information received at the disaster management center, such as the number of injured people, the amount of demand of the affected people, traveling times according to the network conditions and available commodities, etc. are inherently imprecise and uncertain. To avoid any inefficiency in the final selected solutions, such inherent uncertainty in input data should be taken into account. Thus, it is desirable to have optimization models and solution techniques to deal with the multi-objective nature and the uncertainty features of HRC

simultaneously.

Disaster management operations are usually classified into four phases: mitigation and preparedness (pre-disaster), response, and recovery (post-disaster). These four phases together are known as the disaster management cycle (Altay and Green III, 2006). The preparedness and response are relief phases, whereas the mitigation and recovery are development phases. Our problem falls into the disaster relief phases. When a disaster (either a sudden-onset disaster that occurs as a single, distinct event, such as an earthquake or a slow-onset disaster that emerges gradually over time, such as a drought) strikes, relief goods are transported to the points of distributions (PODs) by relief organizations. Then, affected people walk or drive to these centers to collect their relief aid. Since the numbers, as well as the locations of the PODs and their capacity, directly affect the performance of the relief chain in terms of response time and costs (Balcik and Beamon, 2008), facility location decisions in disaster management are of vital importance. This paper deals with a two-stage bi-objective location-allocation problem to design a last-mile relief network where one objective is affected by data uncertainty.

As mentioned before, stochastic programming and robust optimization with different concepts are two widely applied techniques, among others, for modeling decision problems under uncertainty both in single- and multi-stage problems. Now, we might raise the question of which concept performs better in a disaster situation. Our focus is to find an efficient and reliable methodology to address the problem through comparison and interpretation of efficient sets resulting from the combination of the bi-objective model and different concepts of robust and stochastic optimization.

In most of the humanitarian literature addressing uncertainty, either the expected value of a performance measure or worst-case robustness is considered to cope with uncertainty. In this paper, we analyze traditional two-stage risk-neutral stochastic and adaptive (two-stage) robust optimization as well as a two-stage risk-averse stochastic framework which can be seen as a method between the other two approaches using a widely applied risk measure, namely the conditional value-at-risk (CVaR( $\alpha$ )). With the help of uncertainty level  $\alpha$  ( $\alpha \in [0, 1]$ ), it can be adapted to the DM's risk preference. Two-stage stochastic and adaptive robust optimization are two special cases of the CVaR with  $\alpha = 0$  and  $\alpha \approx 1$ , respectively. Towards that end, we employ two linear representations of CVaR: classical representation and subset-based representation of CVaR. Since solving the subset-based formulation is computationally expensive, we propose a scenario decomposition-based algorithm. Additionally, since large-size instances are difficult to solve to optimality, we develop a matheuristic method which finds high-quality approximations of the set of trade-off solutions.

The remainder of this paper is organized as follows. A literature review on uncertain multi-objective problems in the context of HRC is presented in Section 2. In Section 3, we define the uncertain bi-objective facility location problem addressed in this paper and its mathematical formulation. After that, in Section 4, we summarize the developed solution approaches to solve the problem. Section 5 presents and discusses the computational results. Finally, in Section 6 we present conclusion and address potential future works.

## 2 Related work

As mentioned in the Introduction, multiple objectives and uncertainty are two major characteristics of humanitarian decision support systems in practice. Uncertainty, as well as multi-objective optimization, have been considered abundantly in the literature on humanitarian relief. Hoyos et al. (2015) review the literature on operation research models considering stochasticity in disaster response management. Grass and Fischer (2016) survey publications considering two-stage stochastic programming in the context of disaster management. Gutjahr and Nolz (2016) give an extensive review of quantitative multi-criteria decision making in humanitarian aid. The papers published until 2015 are classified based on different criteria, including the way uncertainty is approached and incorporated into multi-criteria decision making. The survey is categorized into pre-disaster and post-disaster phases of disaster relief. According to the authors, capturing uncertainty in multi-criteria optimization is critical in practice and still a comparably young field.

The majority of the studies in the literature that addresses MOO under uncertainty in different phases of disaster relief (e.g., Tzeng et al. (2007), Tricoire et al. (2012), Rath et al. (2016), Najafi et al. (2013), Rezaei-Malek and Tavakkoli-Moghaddam (2014), Hagh et al. (2017), Kinay et al. (2019), Liu et al. (2017)) use either scenario-based traditional two-stage stochastic programming (e.g., Tricoire et al. (2012), Rath et al. (2016)) or scenario-based worst-case robust optimization (e.g., Najafi et al. (2013), Rezaei-Malek and Tavakkoli-Moghaddam (2014), Hagh et al. (2017)) to cope with uncertainty. Noyan (2012) propose risk averse stochastic programming for single-objective problems in disaster management. This work was extended in Noyan et al. (2019) to a multi-criteria optimization approach with a two-stage stochastic programming model. As in our present work, Noyan et al. (2019) use the CVaR to represent risk averseness. However, the multi-criteria decision approach is different from ours, insofar as Noyan et al. (2019) apply the CVaR in the context of multivariate stochastic dominance constraints, whereas we use the concept of Pareto efficiency (the most prominent concept in multi-objective optimization) to determine the trade-off between our considered objective functions. To the best of our knowledge, incorporating risk-averse stochastic programming into multi-objective optimization using Pareto analysis has not been considered in the HRC literature so far. In addition, despite the applicability of the concept of adaptive robust optimization in disaster relief, this concept also has not been considered in the HRC literature.

From a methodological point of view, some of these studies use the  $\epsilon$ -constraint method (Laumanns et al., 2006) to find the optimal *Pareto frontier* (e.g., Tricoire et al. (2012), Rath et al. (2016)), while others develop metaheuristic algorithms to approximate the Pareto frontier for large-size instances (e.g., Hagh et al. (2017)).

One of the first works on uncertain MOO in HRC is done by Tzeng et al. (2007). They propose a fuzzy three objective model for relief distribution systems by pursuing efficiency and fairness goals. They employed fuzzy multi-objective linear programming to reformulate the mathematical model as a single objective model.

Zhan and Liu (2011) propose a bi-objective stochastic programming model for the location-allocation problem in an emergency logistics network. The objectives represent fairness and efficiency in a disaster situation. Demand, supply, and the availability of a path are considered as random parameters. Uncertainty of parameters is handled by chance constraints and scenario planning. Goal programming is used to solve the bi-objective problem.

Tricoire et al. (2012) develop a bi-objective two-stage stochastic model to deal with distribution center selection for relief commodities and delivery planning. The authors consider the demand as a random parameter and approximate them by a sample of randomly generated scenarios. A new solution approach is proposed based on the  $\epsilon$ -constraint method for the computation of the Pareto frontier of the bi-objective problem using a branch-and-cut algorithm. Finally, they test the proposed algorithm using data of a real-world application in Senegal. In this paper, we address the case of Senegal using a different model.

Rath et al. (2016) formulate several variants of a two-stage bi-objective stochastic programming model in the response phase of disasters. They apply the  $\epsilon$ -constraint method to compute the Pareto frontier. They evaluate the benefit of the stochastic bi-objective model in comparison to the deterministic bi-objective model using the value of stochastic solution (VSS) measure.

Najafi et al. (2013) propose a hierarchical multi-objective stochastic model to manage the logistics of earthquake response. They consider the amount of commodities and the number of injured people as uncertain parameters and solve it by means of a robust approach for models with uncertain right-hand sides (Bertsimas et al., 2004). They develop a robust model to assess whether or not the distribution plan performs well under the different scenarios of an earthquake. Finally, an illustrative example is presented to show how the model is capable of capturing all crucial network information and how the solution methodology generates robust solutions in acceptable computation times.

Rezaei-Malek and Tavakkoli-Moghaddam (2014) consider a bi-objective robust problem in the response phase of a disaster. A scenario-based robust approach is used to represent uncertainty of demands, roads, and transportation time in a disaster. The robust optimization method by Mulvey et al. (1995) is chosen to deal with the uncertainty in objective functions and constraints. They use the reservation level Tchebycheff procedure, a modification of the interactive weighted Tchebycheff procedure by Steuer and Choo (1983). Finally, the technique is tested via a real case study in Iran.

Haghi et al. (2017) develop a metaheuristic algorithm for a multi-objective location and distribution model with pre/post-disaster budget constraints for goods and casualties logistics. In order to handle the uncertainties, a robust optimization approach is embedded into the  $\epsilon$ -constraint method. To solve large-size instances, they propose a metaheuristic algorithm that is a combination of a genetic algorithm and simulated annealing (Kirkpatrick et al., 1983). The results are compared to those of the NSGAII (Deb et al., 2002). Then the validity and efficiency of the proposed algorithm is explored in comparison to the exact methods.

Kinay et al. (2019) develop a tri-criteria facility location model for a shelter site location case study in Istanbul, Turkey, with stochastic demand in a disaster context. To deal with uncertain demand,

a chance-constraint model is developed. They deploy vector optimization and goal programming frameworks to find the exact Pareto frontier for the proposed model. Finally, they test the model using two real-world data sets and conclude that considering uncertainty and multiple objectives in this type of facility location problems leads to solutions that may better support decision making.

Parragh et al. (2020) propose an uncertain bi-objective facility location problem considering stochastic demand in disaster relief context. They formulate the uncertainty using a scenario-based two-stage risk-neutral stochastic approach. They integrate the L-shaped method into a bi-objective branch-and-bound framework to deal with the problem. They test and compare different cutting-plane schemes to find the best approximation of Pareto frontiers for a large number of samples.

The focus of our paper is on the evaluation of different combinations of two criterion space search methods, the well-known  $\epsilon$ -constraint (Laumanns et al., 2006) and the recently proposed balanced box (Boland et al., 2015) methods and three different uncertainty approaches, the widely used risk-neutral two-stage stochastic programming approach, adaptive (two-stage) robust optimization and two-stage risk-averse stochastic programming using CVaR. It aims at finding an efficient method to generate the entire Pareto frontier by considering last-mile setting assumptions. It is assumed that the demand of affected people is uncertain.

In addition, a decomposition-based algorithm is proposed to deal with computationally challenging representation of two-stage CVaR model. Furthermore, as it is not possible to solve large-size instances to optimality within a reasonable time limit, we propose an iterative mixed integer programming (MIP)-based matheuristic method.

### 3 Problem description

Due to scarcity of resources, in many disaster relief situations, including slow-onset disasters or sudden-onset disasters, humanitarian organizations encounter challenging logistical *last-mile* operations (Rancourt et al. (2015), Balcik and Beamon (2008)). On the one hand, the humanitarian organizations goal in such a context is to reduce beneficiaries vulnerability by maximizing coverage. On the other hand, they face limited monetary resources and want to reduce their costs. Therefore DMs face two conflicting objectives, and a trade-off solution needs to be identified.

We consider a bi-objective location-allocation problem for a last-mile network, motivated by the drought case studies presented by Tricoire et al. (2012) and Rancourt et al. (2015), as well as the earthquake case presented by Noyan et al. (2016) in which the authors design a last-mile aid distribution network. Unlike Tricoire et al. (2012), the two latter studies rely on a single objective approach, albeit the authors acknowledge and analyze different objectives. The main framework for the cases is the same (Figure 1). The aim is to find the best locations to position temporary PODs in a relief phase of a disaster where beneficiaries walk to these PODs to pick up the aid packages. Two objective functions are considered: the first objective is the minimization of location costs, and the second objective is to minimize the number of uncovered demand of beneficiaries (effectiveness-related

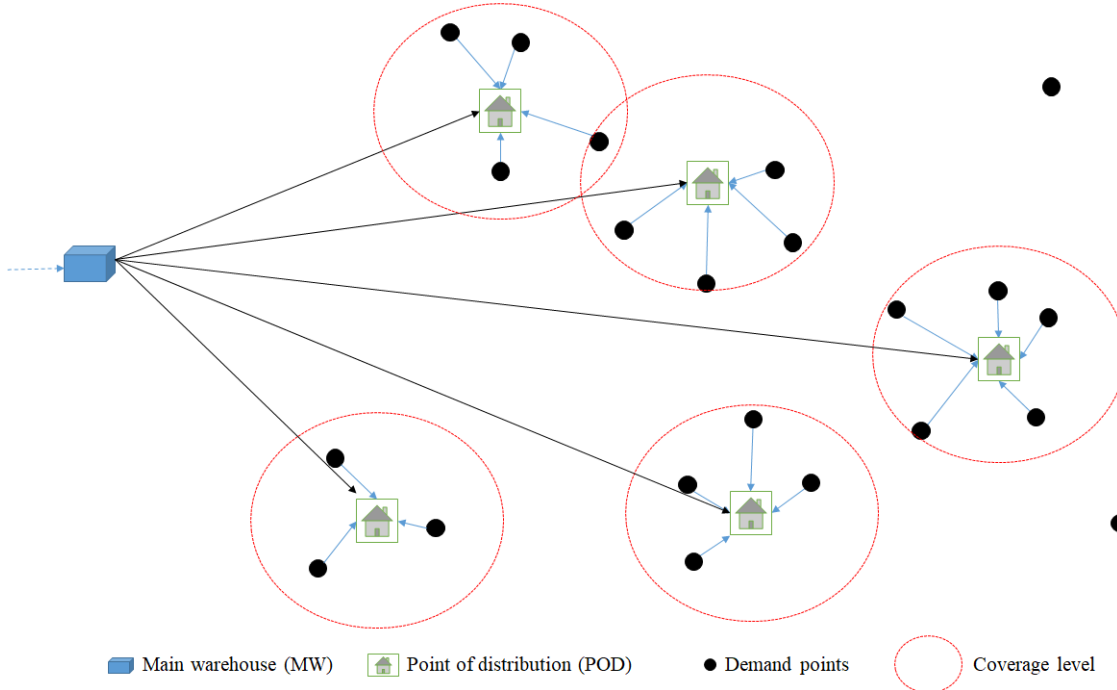


Figure 1: Last Mile Relief Network  
Source. Modified from Noyan et al. (2016)

criterion).

In this paper, we consider the amount of demand as an uncertain parameter, as the demand of the affected people depends on the crisis's intensity which is uncertain (single source of uncertainty). Without loss of generality, the model can also be applied to a disaster context with multiple sources of uncertainty (e.g., the demand of the affected people, the capacity of PODs, the availability of transportation links, etc.).

The problem is formulated on a graph  $G = (V_0, A)$ , where  $V_0$  is the set of nodes, and  $A$  is the set of arcs.  $V_0$  can be partitioned into  $\{\{0\}, I\}$ , where  $\{0\}$  is the main warehouse (MW), supplying the selected PODs, and  $I$  is the set of affected nodes and a superset of the set of potential PODs,  $J$  (Without loss of generality we assume the set of potential PODs is a subset of the set of affected nodes  $J \subseteq I$ : If a potential POD is not affected, it can be represented as a virtual affected node with zero beneficiaries). We assume that the location of the MW is determined before the optimization.

Another assumption is that beneficiaries in each affected location ( $i \in I$ ) will walk only to the one opened POD ( $j \in J$ ), which they are assigned to, in order to fulfill their demand ( $q_i^{(s)}$ ) (single-source assumption). Moreover, beneficiaries will not walk to any PODs, if their distance ( $d_{ij}$ ) from an opened POD is more than a certain distance threshold ( $d_{max}$ ).

The first stage decision (represented by decision variables  $y_j$ ) is the location of PODs with limited capacity ( $c_j$ ) and given fixed cost ( $\gamma_j$ ). This decision has to be made before the realization of the uncertain parameters. The second stage decisions determine the assignments of demand nodes to the opened PODs (decision variables  $x_{ij}^{(s)}$ ) and the amount of relief items delivered to each POD (decision variables  $u_j^{(s)}$ ), which are determined based on first stage decisions and realized uncertain

information. Table 1, summarizes the employed notation.

Table 1: Notation

Sets	
$I$	set of demand nodes
$J$	set of potential PODs, $J \subseteq I$
$S$	set of scenarios
Certain Parameters	
$\gamma_j$	fixed cost to open POD $j \in J$
$c_j$	maximum capacity of POD $j \in J$
$\psi(d_{ij})$	coverage level: 1 if $d_{ij} \leq d_{max}$ , 0 otherwise
Uncertain Parameters	
$q_i^{(s)}$	demand of demand point $i \in I$ under scenario $s \in S$
Decision Variables	
$y_j$	1 if POD $j \in J$ is selected to be open, 0 otherwise
$x_{ij}^{(s)}$	1 if demand point $i \in I$ is assigned to POD $j \in J$ under scenario $s \in S$ , otherwise 0
$u_j^{(s)}$	quantity of supply delivered to POD $j \in J$ under scenario $s \in S$
Objective functions	
$f_1$	first stage objective: Total (location) opening cost
$f_2$	second stage objective: Total amount of uncovered demand (uncertain objective)

### 3.1 Base formulation

In mathematical terms, a nominal formulation of the first stage is the following. Note that the precise meaning of minimizing  $f_2$  is not yet specified, we shall return to this issue in Subsection 3.2.

$$\min f_1 = \sum_{j \in J} \gamma_j y_j \quad (1)$$

$$\min f_2 = Q(y, \xi) \quad (2)$$

$$\text{s.t.} \quad y_j \in \{0, 1\} \quad \forall j \in J \quad (3)$$

Here  $\xi$  denotes the random data and  $Q(y, \xi)$  is the second objective function associated with the second stage of the problem for a given decision resulting from the first stage. It represents the uncovered demand resulting from decision  $y$ , if the uncertain data realize as  $\xi$ . The second stage is formulated as follows for the realization of the random data under scenario  $s \in S$  ( $\xi^s = (q^s)$ ):

$$\min \quad Q(y, \xi^s) = \sum_{i \in I} q_i^{(s)} - \sum_{j \in J} u_j^{(s)} \quad (4)$$

$$\text{s.t.} \quad \sum_{j \in J} \psi(d_{ij}) x_{ij}^{(s)} \leq 1 \quad \forall i \in I \quad (5)$$

$$u_j^{(s)} \leq c_j y_j \quad \forall j \in J \quad (6)$$

$$u_j^{(s)} \leq \sum_{i \in I} q_i^{(s)} \psi(d_{ij}) x_{ij}^{(s)} \quad \forall j \in J \quad (7)$$

$$x_{ij}^{(s)} \leq y_j \quad \forall i \in I, \forall j \in J \quad (8)$$

$$x_{ij}^{(s)} \in \{0, 1\} \quad \forall i \in I, \forall j \in J \quad (9)$$

$$u_j^{(s)} \in \mathbb{Z}^+ \quad \forall j \in J \quad (10)$$

The first objective (1) minimizes opening costs, and the second one (2) minimizes the uncovered demand of the affected people. Constraint (5) indicates coverage constraints. It makes sure that any part of the demand at  $i$  is only covered at most once. Constraints (6) ensure that the capacity of POD  $j$  is not exceeded. Constraints (7) link the coverage variables with the assignment variables: the covered demand with POD  $j$  cannot be higher than the actual demand assigned to this node. Constraints (8) guarantee that a demand node can only be assigned to an opened POD, and finally, constraints (3), (9) and (10) give the domains of the variables.

## 3.2 Uncertainty treatment

To deal with parameter uncertainty, as mentioned in the introduction, we use three different approaches, two-stage risk-neutral stochastic programming (expected value), two-stage (adaptive) robust optimization, and two-stage risk-averse stochastic programming (CVaR). We consider a scenarios-based framework to make a fair comparison among all the above-mentioned approaches. We characterize the uncertainty in parameters via a finite discrete set of random scenarios ( $s \in S$ ,  $S = \{1, \dots, N\}$ ) where each scenario has the same probability ( $\frac{1}{N}$ ). In the following, we provide the corresponding models.

### 3.2.1 Two-stage risk-neutral stochastic optimization

As mentioned before, the nature of the decision-making process in our problem is sequential: the decision on the location of the POD has to be taken before the realization of uncertain data. The assignment of demand points to an opened POD is done afterwards. We capture this setting through a two-stage stochastic programming model and in a risk-neutral context by taking the expected value of the random variable  $f_2$  as the evaluation of second-stage costs. Representing the probability distribution by  $N$  equiprobable scenarios as described above, the second-stage objective function ( $f_2$ ) will be replaced by the expected value of the uncovered demand in the stochastic model. So, the

gained deterministic counterpart of the bi-objective model (1) to (10) is as follows (**M1**):

$$\min \sum_{j \in V} \gamma_j y_j \quad (11)$$

$$\min E(Q(y, \xi^s)) = \frac{1}{N} \sum_{s \in S} \left( \sum_{i \in V} q_i^{(s)} - \sum_{j \in V} u_j^{(s)} \right) \quad (12)$$

$$\text{s.t.} \quad (3), (5) - (10)$$

### 3.2.2 Adaptive robust optimization

The above two-stage stochastic approach is based on the expected value, whereas minmax robustness is based on the worst-case scenario (pessimistic view). Adaptive robust optimization, in which the recourse function is a worst-case value over a set of scenarios (also called minimax two-stage stochastic programming), might give less conservative solutions according to Bertsimas et al. (2010) who compared to static (minmax) robustness. By replacing  $f_2$  with its worst value in (1)-(10), the deterministic counterpart of the bi-objective model is as follow (**M2**):

$$\min \sum_{j \in V} \gamma_j y_j \quad (13)$$

$$\min \max_{s \in S} (Q(y, \xi^s)) = \sum_{i \in V} q_i^{(s)} - \sum_{j \in V} u_j^{(s)} \quad (14)$$

$$\text{s.t.} \quad (3), (5) - (10)$$

### 3.2.3 Two-stage risk-averse stochastic optimization

So far, to cope with randomness in our problem, we have employed the expected value of coverage, which corresponds to a risk-neutral approach, and the worst-case value of the coverage, which is the adaptive robustness approach. These two approaches are at the two ends of the risk averseness spectrum, in which the risk-neutral approach gives a comparably optimistic view whereas the adaptive robust approach represents a pessimistic view of the random outcome. Sometimes, DMs are not risk-neutral, but less risk-averse than assumed by the adaptive robust approach. For these cases, we consider a two-stage risk-averse stochastic optimization model where the degree of risk-aversion can be specified. We use the widely applied conditional value-at-risk (CVaR) as the risk measure in our study which leads to a computationally tractable model.

In this paper we employ two linear representations of CVaR that are valid on the assumption of an underlying finite discrete probability space: classical representation and subset-based representation of CVaR.

**The classical representation of CVaR (CCVaR)** Let us start by briefly discussing the concept of the CVaR, and then present its classical mathematical representation. The precise definition of CVaR at confidence level  $\alpha \in [0, 1)$  of a random variable  $X$  is given by Rockafellar et al. (2000) as follows:

$$\text{CVaR}_\alpha(X) = \min\{\eta + \frac{1}{1-\alpha}E([X - \eta]_+) : \eta \in \mathbb{R}\}, \quad (15)$$

Therein,  $[b]_+ = \max\{b, 0\}$ ,  $b \in \mathbb{R}$  and  $\eta$  is the Value-at-Risk,  $\text{VaR}_\alpha(X)$ , of variable  $X$  at confidence level  $\alpha$ . It is defined as follows, where  $F_X(\cdot)$  is the cumulative distribution function of a random variable  $X$ .

$$\text{VaR}_\alpha(X) = \min\{\eta \in \mathbb{R} : F_X(\eta) \geq \alpha\}, \quad (16)$$

$\text{CVaR}_\alpha(X)$  can be interpreted as the conditional expected value exceeding the VaR at the confidence level  $\alpha$  (see, Rockafellar et al. (2000)).

The auxiliary real variables  $w_s$  for  $s = 1, \dots, N$  are introduced to reduce (15) to a linear programming problem:

$$\min \quad \text{CVaR}_\alpha(X) = \eta + \frac{1}{1-\alpha} \frac{1}{N} \sum_{s=1}^N w_s \quad (17)$$

$$\text{s.t.} \quad w_s \geq X - \eta \quad \forall s = 1, \dots, N \quad (18)$$

$$w_s \geq 0 \quad \forall s = 1, \dots, N \quad (19)$$

$$\eta \in \mathbb{R} \quad (20)$$

In our problem, we calculate the CVaR value for the second-stage objective  $Q(y, \xi^s)$  with  $s = 1, \dots, N$ . The deterministic equivalent formulation of our model is as follows (**M3A**):

$$\min \quad \sum_{j \in V} \gamma_j y_j \quad (21)$$

$$\min \quad \text{CVaR}_\alpha(Q(y, \xi^s)) = \eta + \frac{1}{1-\alpha} \frac{1}{N} \sum_{s \in S} w_s \quad (22)$$

$$\text{s.t.} \quad w_s \geq Q(y, \xi^s) - \eta \quad \forall s \in S \quad (23)$$

$$w_s \geq 0 \quad \forall s \in S \quad (24)$$

$$\eta \in \mathbb{R} \quad (25)$$

$$(3), (5) - (10)$$

This formulation is equivalent to the two-stage stochastic (expected value) approach in the special case  $\alpha = 0$ , and it is equivalent to the adaptive (two-stage) robust approach for sufficiently large value of  $\alpha$ ,  $\alpha \rightarrow 1$ .

**Two-stage subset-based CVaR approach (SSCVaR)** Fábián (2008) obtains a polyhedral subset-based representation of the classical CVaR for the special case of scenarios with equal probabilities where  $\alpha = 1 - \frac{k}{N}$ ;  $k$  is the cardinality of any subset of scenarios. The cardinality of all scenarios is equal to  $N$  (i.e.,  $\bar{S} \subseteq S, |\bar{S}| = k$ ):

$$\text{CVaR}_{1-\frac{k}{N}}(X) = \frac{1}{k} \max_{\bar{S} \subseteq S : |\bar{S}| = k} \sum_{s \in \bar{S}} X^{(s)} \quad (26)$$

where  $X^{(s)}$  is the value of the random variable  $X$  in scenario  $s$ . Equation (26) leads to the following subset-based polyhedral representation of CVaR (Fábián (2008)):

$$\text{CVaR}_{1-\frac{k}{N}}(X) = \left\{ \min \varrho : \varrho \geq \frac{1}{k} \sum_{s \in \bar{S}} X^{(s)}, \forall \bar{S} \subseteq S : |\bar{S}| = k \right\} \quad (27)$$

We utilize the subset-based representation (27) to obtain the MIP formulation of our two-stage model **(M3B)**:

$$\min \quad \sum_{j \in V} \gamma_j y_j \quad (28)$$

$$\min \quad CVaR_\alpha(Q(y, \xi^s)) = \varrho \quad (29)$$

$$\varrho \geq \frac{1}{k} \sum_{s \in \bar{S}} Q(y, \xi^s) \quad \forall \bar{S} \subseteq S : |\bar{S}| = k \quad (30)$$

$$\varrho \geq 0 \quad (31)$$

$$\text{s.t.} \quad (3), (5) - (10)$$

## 4 Solution approach

In this section, we first define solution concepts in a multi-objective setting. Thereafter, we describe two exact bi-objective frameworks that are used to solve small instances. Then, we propose a matheuristic method to deal with large-size instances. It uses the MIP as a backbone and a local search algorithm to heuristically generate better solutions.

Furthermore, we design a decomposition-based method to deal with a large number of subsets in model M3B, as a large number of subsets in M3B makes solving it more challenging. It generates a

close to optimal Pareto frontier.

## 4.1 Multi-objective concepts and definitions

Due to the bi-objective nature of our problem, it is not possible to find a unique optimal solution, but rather the so-called set of efficient solutions. A MOO problem is given as follow:

$$\min_{x \in X} \quad f(x) = (f_1(x), f_2(x), \dots, f_m(x)) \quad (32)$$

Therein,  $m \geq 2$  is the number of objectives,  $x \in X$ , where  $X$  is the set of feasible solutions in the *decision space* and functions  $f_i : X \rightarrow \mathbb{R}$  are the objective functions, and  $Z = f(X)$  the image of the set of feasible solutions in the *criterion space*.

### Definition 4.1. Pareto dominance

Solution  $x^* \in X$  dominates  $x \in X$  if and only if  $x^*$  is as good as  $x$  with respect to all objectives, and better than  $x$  with respect to at least one of the objectives, i.e.,

$$\begin{cases} f_i(x^*) \leq f_i(x) & \text{for all } i \in \{1, \dots, m\} \\ f_j(x^*) < f_j(x) & \text{for at least one } j \in \{1, \dots, m\} \end{cases}$$

### Definition 4.2. Pareto frontier

$x \in X$  is an efficient solution of MOO (32) if there is no  $x^* \in X$  that dominates  $x$ . The set of efficient solutions of MOO is denoted by  $X_e$ . The objective vector  $f(x)$  of an efficient solution  $x \in X_e$  is called non-dominated solution, and  $Z = f(X_e) = \{f(x) : x \in X_e\}$  is the set of non-dominated objective points (NDP) or Pareto frontier.

## 4.2 Multi-objective exact solution techniques

Most of the papers in the literature of HRC have deployed metaheuristic techniques to solve large-size (i.e., real-world) instances of mathematical models. Metaheuristic techniques cannot provide performance guarantees, whereas exact methods can. Among exact methods, criterion space search methods (i.e., methods that search in the space of objective function values) are often computationally more efficient than decision space search methods (i.e., methods that search in the space of feasible solutions) (Boland et al., 2015). To find a good approximation of the entire Pareto frontier, we employ two criterion space search frameworks, the well-known  $\epsilon$ -constraint method due to its simplicity (Laumanns et al., 2006) and the recently developed balanced box method (Boland et al., 2015) since it has been shown that it performed well for large-size problems. It is worth noting that these frameworks are exact algorithms that give an approximation of the Pareto frontier if they are

terminated before completion, e.g. if a tight time limit is employed.

The  $\epsilon$ -constraint method generates all NDPs step by step iteratively. Let us describe the method for the special case  $m = 2$ . It starts by finding the endpoints of the Pareto frontier using lexicographic optimization. Lexicographic optimization is performed as follows: we optimize the first objective function ( $f_1$ ) and gain the optimal minimum value  $f_1 = f_1^{min}$ . Then, we optimize the second objective function ( $f_2$ ) by adding constraint  $f_1 = f_1^{min}$  to the model in order to keep the optimal solution value of the first optimization and  $f_2^{max}$  is obtained. The solution to this procedure gives the first extreme point ( $Z^T$ ). This procedure can be represented in the following notation (note that  $R(z^1, z^2)$  is the box in the criterion space defined by the points  $z^1 = (f_1^1, f_2^1)$  and  $z^2 = (f_1^2, f_2^2)$  where  $f_1^1 \leq f_1^2$  and  $f_2^2 \leq f_2^1$ ):

$$Z^T = \text{lexmin}\{f_1, f_2 : f \in R((-\infty, \infty), (\infty, -\infty))\} \quad (33)$$

The second extreme point ( $Z^B$ ) is found by optimizing the second objective function ( $f_2$ ) and obtaining the optimal minimum value  $f_2 = f_2^{min}$ . Then, the first objective function ( $f_1$ ) is optimized by adding constraint  $f_2 = f_2^{min}$  to the model and  $f_1^{max}$  is gained:

$$Z^B = \text{lexmin}\{f_2, f_1 : f \in R((-\infty, \infty), (\infty, -\infty))\} \quad (34)$$

The  $\epsilon$ -constraint algorithm enumerates each NDP one by one from the direction of one endpoint to the other. In all iterations, one and the same of the objective functions is considered as the main objective and the other in terms of an  $\epsilon$ -constraint. The parameter  $\epsilon$  is set as given in lines 5 and 7 in Algorithm 1. Since the objectives take integer values in our problem, the smallest difference value ( $d$ ) is 1.

We note that the choice of direction in the  $\epsilon$ -constraint method can play an essential role in the performance of the algorithm. In our case, we optimize  $f_2$  as the main objective and handle  $f_1$  in the  $\epsilon$ -constraint based on preliminary results. That is, the Pareto solutions are enumerated from  $Z^B$  to  $Z^T$ . Algorithm 1 shows the procedure of the  $\epsilon$ -constraint framework.

---

**Algorithm 1**  $\epsilon$ -constraint framework

---

```

1: input :  $Z^T = (f_1^{min}, f_2^{max}), Z^B = (f_1^{max}, f_2^{min})$ 
2:  $L \leftarrow \emptyset$ 
3:  $\epsilon \leftarrow f_1^{max} - d$ 
4: repeat
5:    $x \leftarrow \text{lexmin}\{f_2, f_1 : f_1 \leq \epsilon\}$ 
6:    $L \leftarrow L \cup x$ 
7:    $\epsilon \leftarrow f_1(x) - d$ 
8: until  $\epsilon \geq f_d^{min}$ 
9: return  $L$ 

```

---

On the other hand, the balanced box method keeps a priority queue of boxes in criterion space in

non-decreasing order of their areas. In the beginning, the priority queue is empty. So, similar to the  $\epsilon$ -constraint method, the algorithm first finds the endpoints of the Pareto frontier  $(Z^T, Z^B)$ . These two points define the initial box  $R(Z^T, Z^B)$ . It contains all not yet found NDPs. Subsequently, all the other boxes are generated and explored iteratively.

In each iteration, the largest box in the priority queue pops out, and the algorithm then splits the box horizontally into two equal parts  $R^T$  and  $R^B$ . It first explores the bottom box for a NDP by optimizing the first objective function. It then explores the top box for a NDP with minimization of the second objective function. The procedure can be repeated until no more boxes are left unexplored in the priority queue. The pseudocode of this framework is presented in Algorithm 2.

---

**Algorithm 2** Balanced box framework

---

```

1: input :  $Z^T = (f_1^{min}, f_2^{max}), Z^B = (f_1^{max}, f_2^{min})$ 
2:  $L \leftarrow \emptyset$ 
3:  $P \leftarrow R(Z^T, Z^B)$ 
4: while  $P \neq \emptyset$  do
5:    $R^B \leftarrow R((f_1^{min}, (\frac{f_2^{min}+f_2^{max}}{2})), Z^B)$ 
6:    $\bar{Z}^T \leftarrow \text{lexmin}(f_1, f_2, f \in R^B)$ 
7:   if  $\bar{Z}^T \neq Z^B$  then
8:      $L \leftarrow L \cup \bar{Z}^T$ 
9:      $P \leftarrow P \cup R(\bar{Z}^T, Z^B)$ 
10:  end if
11:   $R^T \leftarrow R(Z^T, (\bar{Z}^T - \delta))$ 
12:   $\bar{Z}^B \leftarrow \text{lexmin}(f_2, f_1, f \in R^T)$ 
13:  if  $\bar{Z}^B \neq Z^B$  then
14:     $L \leftarrow L \cup \bar{Z}^B$ 
15:     $P \leftarrow P \cup R(Z^T, \bar{Z}^B)$ 
16:  end if
17: end while
18: return  $L$ 

```

---

### 4.3 A matheuristic solution algorithm

Although small instances can be solved to optimality by the exact solution techniques, we develop a matheuristic method to compute high-quality approximated Pareto frontiers for the large-size instances. It combines the  $\epsilon$ -constraint method and a local branching framework to speed up the computationally expensive part of the  $\epsilon$ -constraint method.

Local branching (Fischetti and Lodi, 2003) is a general MIP-based framework which explores a neighborhood of a feasible reference solution  $\bar{y}$  to identify a better solution. Assume  $\bar{A} = \{j \in V : \bar{y}_j = 1\}$  is the set of indices of potential POD variables where their value is equal to one. To construct a  $l$ -OPT neighborhood  $N(\bar{y}, l)$  of the reference solution, the following local branching constraint is added to the model:

$$\sum_{j \in \bar{A}} (1 - y_j) + \sum_{j \in V \setminus \bar{A}} y_j \leq l \quad (35)$$

Constraint (35) states that at most  $l$  variables of the reference solution  $\bar{y}$  switch their values either from 1 to 0 or from 0 to 1.

Not that the cardinality of the binary support of any feasible solution is a constant in our model. Therefore, constraint (35) can equivalently be written in its *asymmetric* form:

$$\sum_{j \in \bar{A}} (1 - y_j) \leq l' \quad (36)$$

This framework, embedded into an  $\epsilon$ -constraint procedure, can explore the neighborhood of every single NDP in the criterion space. More precisely, local branching is added to an NDP where the cost of uncovered demand  $f_2$  is the main objective and  $f_1$  which is the opening cost of the selected PODs ( $y_j$ ) is treated as the  $\epsilon$ -constraint.

However, we adapt it to make use of problem-specific features. Comparing the properties of NDPs along the Pareto frontier of instances solved to optimality leads to the following observations: Moving along the frontier solution by solution from one end-point ( $Z^B$ ) to the other one ( $Z^T$ ), very often one of the opened facilities (i.e.,  $y_j = 1$ ) is closed, and the set of closed facilities is kept unchanged (i.e.,  $y_j = 0$ ). However, there is a significant difference between the first and the second efficient solutions along the frontier, not only in terms of the number of differences in  $y_j$  values (i.e., more than one open/closed facility) but also in terms of run time.

Therefore, we developed the following procedure in order to find a high-quality approximation of the Pareto frontier: (i) we find the optimal Pareto efficient endpoints ( $Z^T$  and  $Z^B$ ), (ii) noting that we move along the frontier in the direction from  $Z^B$  to  $Z^T$  in our  $\epsilon$ -constraint method, we approximate the second efficient solution (adjacent with  $Z^B$ ) by solving the linear relaxation of the model and deploying local branching to speed up the algorithm, (iii) we generate the rest of the Pareto frontier iteratively by fixing variables of closed facilities (i.e.,  $y_j = 0$ ) derived from the previously enumerated solution.

#### 4.4 Scenario subset-based approximation

Formulation M3B contains constraints corresponding to subsets of  $S$ . The size of this set of constraints could grow fast, depending on the cardinality of the subset ( $k$ ) and  $S$ . Hence, we develop a decomposition-based technique to efficiently solve M3B and generate a good-quality approximation of the Pareto frontier.

Different decomposition-based techniques have been proposed to solve two-stage stochastic programming models with a single objective (e.g., Shapiro et al., 2009). Noyan (2012) propose a Benders decomposition-based framework for the subset-based variant of CVaR with a mean-risk objective function. In the classical single objective two-stage stochastic model, the model is decomposed by scenario once the first-stage variables are fixed.

In our bi-objective setting, due to the presence of integer variables not only in the first stage,

but also in the second stage, using decomposition techniques for every single point along the Pareto frontier causes computationally no benefit. However, preliminary tests showed us that, employing the decomposition algorithm in order to calculate the first extreme point of the Pareto frontier ( $Z^T$ ) and, consequently, adding the generated subset cuts to the model, leads to a better approximation of the entire Pareto frontier.

In our scenario subset decomposition-based approach, we iteratively solve the so-called single objective master problem (relaxed master problem - RMP) which relaxes the subset-based constraints (30), and iteratively generates them using a delayed cut generation algorithm. To be more precise, the single objectives RMP for the  $t$  subsets of  $S$  with a cardinality of  $k$  is as follow:

$$\min \quad \varrho \quad (37)$$

$$\varrho \geq \frac{1}{k} \sum_{s \in \bar{S}_\iota} \theta^s \quad \forall \bar{S}_\iota \subseteq S : |\bar{S}_\iota| = k, \iota = 1, \dots, t \quad (38)$$

$$\varrho \geq 0 \quad (39)$$

$$\theta^s \geq 0 \quad \forall s \in S \quad (40)$$

$$\text{s.t.} \quad (3), (5) - (10)$$

Given an optimal solution  $(\hat{y}, \hat{\varrho}, \hat{\theta})$  of RMP, we check whether there is any violated constraint of the type (38), and identify a subset  $\hat{S}$  if there is a violation. To solve the *separation* problem to find the violated constraint, a few simple calculations are required. It is executed when the algorithm ensures that there is no missing optimality cut. Since CVaR is part of the second stage objective function, no feasibility cut is needed. At this stage, we have the exact optimal second stage objective values associated with the current  $(\hat{y}, \hat{\varrho}, \hat{\theta})$  vector; in particular, these objective values can be expressed as  $\varrho^s = \frac{1}{k} \theta^s$  for all  $s \in S$ . Let  $S^* = \{s \in S : \sum_{s \in S^*} \varrho^s > \hat{\varrho}\}$ . If  $S^* = \{s \in S : \sum_{s \in S^*} \varrho^s \leq \hat{\varrho}\}$  then the candidate solution is labeled as the new incumbent. Otherwise, the identified violated constraint of the form (38) associated with  $S^*$  is introduced as a cutting-plane. The pseudo-code of the delayed cut generation algorithm is presented in Algorithm 3.

**Initial cut** We propose a heuristic algorithm in order to initialize the RMP. This procedure is based on the following steps:

1. Rank the scenarios in each demand point based on their corresponding demand value ( $q_j^s$ ) in descending order.
2. Sum the ranks for each scenario over  $I$ , the set of demand points
3. Sort the scenarios based on their cumulative total rank in descending order
4. Select the first  $k$  scenarios of the sorted set

---

**Algorithm 3** Delayed cut generation

---

```
1: initialize the RMP with the initial cut,  $t \leftarrow 1$ 
2: while  $\sum_{s \in \hat{S}_1} \varrho^s > \hat{\varrho}$  do
3:   for each  $s \in S$  do
4:      $\varrho_s \leftarrow \frac{1}{k} \sum_{i \in V} q_i^{(s)} - \sum_{j \in V} u_j^{(s)}$ 
5:     (sort  $\varrho_s$  in descending order)
6:   end for
7:    $S^* \leftarrow$  the first  $k$  values (largest) of the sorted  $\varrho_s$  values
8:    $\hat{S}_1 \leftarrow S^*$ 
9:    $t \leftarrow t + 1$ 
10: end while
```

---

## 5 Computational study

In the following, we present the computational experiments conducted to evaluate the performance of the proposed methods. We first describe the test instances and then, the quality indicators employed to assess the performance of the methods. This is followed by a recapitulation of the expected value of perfect information (EVPI), and the value of stochastic solution (VSS) used to show the value of incorporating risk measurement. Thereafter, we discuss the computational results.

All experiments have been implemented in C++ using the Concert Technology component library of IBM ILOG CPLEX 12.9 as a MIP solver when multi-threading is disabled. A time limit (TL) of 7200 s has been applied. We note that we use the Generic callback feature of CPLEX in order to generate the cuts in the M3B model. Unlike lazy constraint callback that prevents CPLEX from utilizing dynamic search, Generic callback allows CPLEX to choose among the options of dynamic search and classical branch-and-cut as it suits.

### 5.1 Test instances

To test and evaluate the integration of the above-mentioned uncertainty approaches into the stated multi-objective frameworks, we generate a data set inspired by a real-world study for a slow-onset drought case presented in Tricoire et al. (2012). Tricoire et al. (2012) provided a data set from the region of Thies in western Senegal. Senegal is a developing country in sub-Saharan Africa where droughts occur frequently. Politically, the region is split into 32 rural areas where each contains between 9 and 31 villages (demand nodes). In total, the region contains 500 nodes. In order to test the performance of the proposed solution approaches, we create new networks and artificially generate larger instances with between 21 and 500 nodes by aggregating the demand nodes in the region. For example, the first instance contains 21 nodes, and the second one has 44 nodes, i.e., an instance with 23 nodes is added to the first 21 nodes. Our data set contains 23 test instances.

The distance matrix is obtained by road distances between each pair of nodes. Opening costs for PODs are assumed to be identical for all demand locations (5000 cost units). We also assume that the affected people in a demand node will walk to the closest POD if the distance is less than 6km. We start by considering 10 sample scenarios ( $|S|=10$ ) to cope with demand uncertainty. Thereafter,

to assess the algorithms for a larger number of scenarios, samples with 100, 500, and 1000 scenarios are generated. We refer to Tricoire et al. (2012) for further details.

## 5.2 Solution quality indicators

Different quality indicators for multi-objective approximation algorithms have been proposed in the literature. Zitzler et al. (2003) review the existing quality measures. We employ two of these measurements, namely the hypervolume indicator and the multiplicative  $\epsilon$ -indicator, to assess the performance of the proposed methods.

Given a bi-objective framework with minimization objective functions, let  $X$  be the set of feasible solutions in decision space and  $Z = f(X)$  be the set of feasible solutions in criterion space. We assume  $A \subseteq Z$  is an approximation set of a Pareto frontier, and  $R \subseteq Z$  is a reference set, e.g., the true Pareto frontier.

The hypervolume indicator ( $I_H$ ) (Zitzler and Thiele, 1998) computes the area of the portion of the criterion space, which is weakly dominated by approximation set  $A$  with respect to a reference point (e.g., the Nadir point). The complete Pareto frontier generally has a maximum value of  $I_H$ . The higher the value of  $I_H$ , the higher is the quality of the approximated Pareto frontier. In this paper, for approximation methods, we also introduce a hypervolume gap (gH) indicator given that the entire Pareto frontier ( $R$ ) is known for the instances. Its definition is as follows:

$$gH\% = \frac{I_H(R) - I_H(A)}{I_H(R)} * 100 \quad (41)$$

The closer the value of gH% to 0, the higher is the quality of the approximated Pareto frontier.

The multiplicative epsilon indicator ( $I_\epsilon$ ) (Zitzler et al., 2003) gives the minimum number  $\epsilon$  that the approximation set in the criterion space has to be multiplied with, such that it dominates the reference set. The two-dimension  $I_\epsilon$  is calculated as follows, where all the objectives are positive:

$$I_\epsilon(A, R) = \inf_{\epsilon \in \mathbb{R}} \{ \forall z^2 \in R \ \exists z^1 \in A : z^1 \geq_{\epsilon} z^2 \} \quad (42)$$

The closer the value of  $I_\epsilon$  to 1, the better is the approximated Pareto frontier. The  $\epsilon$  value calculated here can be interpreted as the gap between  $A$  and  $R$  in the criterion space.

## 5.3 Value of using a risk measure stochastic model

Due to the computational challenges of decision making under uncertainty, one of the first questions that DMs might come up with is whether it pays off to consider a stochastic instead of a deterministic model. An answer can be given by using two well-known measures: the expected value of perfect information (EVPI) and the value of stochastic solution (VSS). These measures assess the value of

using a single objective two-stage risk-neutral programming model (see, Birge and Louveaux (2011)).

In this section, we start by recalling these two measures. After that, similarly as in Noyan (2012) where the measures are extended to a single-objective two-stage mean-risk model involving the CVaR, we adapt these concepts to our bi-objective two-stage CVaR model.

The EVPI measures the expected gain of perfect information over the stochastic solution. It is the difference between the wait-and-see solution (WS) and the solution obtained by solving the risk-neutral stochastic model referred to as the recourse problem (RP). WS is obtained by solving the model for each scenario as realized data with a probability of 1, and then taking the expected objective function value:

$$\text{WS} = E(Q(\bar{y}(\xi^s), \xi^s)) \quad (43)$$

Therein,  $\bar{y}(\xi^s)$  denotes the optimal solution of the individual problem for each scenario. Then, by definition:  $\text{EVPI} = \text{RP} - \text{WS}$ .

On the other hand, the VSS evaluates the stochastic model in comparison to an expected value solution, where the latter is defined as the solution of the deterministic problem obtained by replacing each random parameter by its expected value. The VSS is calculated as the difference between the RP solution value and the solution value EEV of the expected value problem. EEV is obtained by solving a deterministic expected value scenario problem in the first step. Then, the resulting optimal first-stage variables are saved and fixed in the model, and the second stage is solved:

$$\text{EEV} = E(Q(\bar{y}(\bar{\xi}), \xi^s)) \quad (44)$$

Where,  $\bar{\xi} = E(\xi^s)$ , and  $\bar{y}(\bar{\xi})$  is the the expected value solution. Then, VSS is calculated as follow:  $\text{VSS} = \text{EEV} - \text{RP}$ .

As it is mentioned, these two measures are based on expected values which are used to assess a risk-neutral stochastic model. However, they cannot be used directly to evaluate a two-stage risk-averse stochastic model. Therefore, we adapt these measures and apply the risk function (CVaR) instead of the expected value in computing the WS and EEV approach. More precisely, we use the following measures for the two-stage CVaR model at the risk level of  $\alpha$  (see, Noyan (2012)):

$$\text{RVPI}(\alpha) = \text{RRP}(\alpha) - \text{RWS}(\alpha) \quad (45)$$

$$\text{RVSS}(\alpha) = \text{REV}(\alpha) - \text{RRP}(\alpha) \quad (46)$$

Therein,  $\text{RRP}(\alpha)$  is the solution obtained by solving the risk-averse CVaR model at the risk level of  $\alpha$ ,  $\text{RWS}(\alpha) = \text{CVaR}_\alpha(Q(\bar{y}(\xi^s), \xi^s))$  is obtained by solving the model for each scenario as realized

data with a probability of 1 and then taking the CVaR objective function value at the risk level of  $\alpha$ , and  $\text{REV}(\alpha) = \text{CVaR}_\alpha(Q(\bar{y}(\bar{\xi}), \xi^s))$  is obtained by solving a deterministic expected value scenario problem in the first step. Then, the resulting optimal first-stage variables are saved and fixed in the model, and the second stage of the risk-averse model is solved at the risk level of  $\alpha$ .

RVPI measures the gain of perfect information based on the CVaR value of the objective values obtained from WS solutions. The RVSS measures the gain from solving the risk-averse model with a specific risk preference. The higher the values of RVSS, the more is the value-added of considering a risk-averse model instead of a risk-neutral problem.

In order to employ these measures to our bi-objective model, we apply them to each non-dominated solution where  $f_1$  is bounded as  $\epsilon$ -constraint, and  $f_2$  is the main objective.

## 5.4 Results

In this section, we conduct numerical experiments to assess the proposed approaches. We compare all combinations;  $\epsilon$ -constraint (e), balanced box (BB) frameworks, and proposed matheuristic (Mat) integrated into deterministic counterparts of the M1, M2, M3A, and M3B models. Let  $\{\text{e-M1}, \text{BB-M1}, \text{e-M2}, \text{BB-M2}, \text{e-M3A}, \text{BB-M3A}, \text{Mat-M3A}, \text{e-M3B}, \text{BB-M3B}, \text{Mat-M3B}\}$  denote the set of all methods considered in this study. Since special cases of M3A and M3B models are identical with M1 and M2 models, we just address the performance of Mat method integrated with the M3A and M3B models.

We first study the combinations of exact multi-objective methods with two widely used uncertainty approaches, two-stage stochastic, and two-stage robust approach (e-M1, BB-M1, e-M2, BB-M2). Then, we compare the performance of their deterministic counterpart with two-stage CVaR deterministic counterpart in its two special cases where  $\alpha = 0$  (risk-neutral) and  $\alpha = 0.9$  (where  $|S|=10 \rightarrow$  the worst value of  $\alpha = 1 - \frac{1}{10} = 0.9$ ). Later, we address the combination of exact and matheuristic multi-objective methods to two variants of two-stage CVaR for different levels of risk (e-M3A, BB-M3A, Mat-M3A, e-M3B, BB-M3B, Mat-M3B).

Table 2 indicates the run time of e-M1, BB-M1, e-M2, BB-M2, e-M3A, BB-M3A in seconds for different instances. TL indicates that the run-time limit, which we fixed as 7200 s, is reached.

As can be seen from Table 2 the combination of the  $\epsilon$ -constraint framework with M1 model (e-M1) finds the complete Pareto frontier even for rather large instances. Furthermore, the deterministic counterpart of two-stage risk-neutral stochastic (M1) and adaptive robust (M2) models outperform the deterministic counterpart of the CVaR model in its special cases ( $\alpha=0$  and  $\alpha=0.9$ ).

Table 2: Run time comparison for M1, M2 and their equivalent special cases of M3A model with  $\alpha=0$  and  $\alpha=0.9$  combined with exact algorithms for test instances of size 21-500 with sample size 10

#Node	$\alpha$ value							
	0				0.9			
	e-M1	BB-M1	e-M3A	BB-M3A	e-M2	BB-M2	e-M3A	BB-M3A
21	1	1	1	2	2	2	2	2
44	16	16	16	22	21	22	20	26
56	18	20	24	31	20	23	19	33
72	28	29	36	51	61	68	64	103
90	56	59	62	110	98	110	99	179
106	115	120	123	229	226	290	210	380
120	128	132	143	241	139	175	138	262
163	421	442	445	818	769	910	636	1365
182	522	559	577	TL	1555	1970	1326	2548
203	820	1050	956	2078	541	652	515	TL
254	5821	TL	6103	TL	TL	TL	TL	TL
264	1950	2590	3903	6800	TL	TL	TL	TL
275	5499	TL	7133	TL	TL	TL	TL	TL
295	TL	TL	TL	TL	TL	TL	TL	TL
326	TL	TL	TL	TL	TL	TL	TL	TL
355	TL	TL	TL	TL	TL	TL	TL	TL
388	TL	TL	TL	TL	TL	TL	TL	TL
410	TL	TL	TL	TL	TL	TL	TL	TL
436	TL	TL	TL	TL	TL	TL	TL	TL
449	TL	TL	TL	TL	TL	TL	TL	TL
472	TL	TL	TL	TL	TL	TL	TL	TL
482	TL	TL	TL	TL	TL	TL	TL	TL
500	TL	TL	TL	TL	TL	TL	TL	TL

Next, we show the computational results for the M3A model obtained on different levels of  $\alpha$  integrated into two exact multi-objective frameworks (Table 3). These results also indicate that a combination of different  $\alpha$  levels with the  $\epsilon$ -constraint method performs better than their combination with the BB technique.

A run time comparison of the two different representations of the CVaR approach, M3A, and M3B, is shown in Table 4. M3A is solved to optimality, whereas M3B is solved using the explained decomposition-based technique to approximate its Pareto frontier. The results for the two special cases of  $\alpha$  (identical with M1 and M2), and one middle level and their corresponding  $k$ -values ( $\alpha = 1 - \frac{k}{N}$ ) are reported. Although the results confirm the previous finding, the combination of the BB and approximately solved M3B method performs slightly better and solves a few more instances within the time-limit.

After analyzing the two exact multi-objective techniques, we apply the proposed matheuristic method to the M3A and M3B models in order to solve the test instances. As indicated in Table 5, contrary to the exact methods, the Mat method successfully solves all the instances within the given time-limit and finds an approximation of the entire Pareto frontier. Additionally, we solve a few instances with a larger number of scenarios. Table 6 shows that the approximately solved representation of the CVaR method (M3B) pays off when the number of scenarios increases.

Computational results of the performance measurements are summarized in Tables 7, 8, 9, and 10. Table 7 details the performance of the  $\epsilon$ -constraint method, the BB method, and the Mat method on all of the instances. We report the number of found NDPs and the  $I_H$  values. For this purpose, we compute the nadir point as a reference point by calculating the worst objective values over the

Table 3: Run time comparison for M3A model combined with exact algorithms and different level of  $\alpha$  for test instances of size 21-500 with sample size 10

$\alpha$ value										
#Node	0		0.2		0.5		0.7		0.9	
	e-M3A	BB-M3A								
21	1	2	1	2	2	2	2	1	2	2
44	16	22	17	23	18	26	17	23	20	26
56	24	31	22	40	21	40	18	22	19	33
72	36	51	37	54	42	59	45	48	64	103
90	62	110	66	119	70	135	73	78	99	179
106	123	229	120	238	128	239	151	161	210	380
120	143	241	136	263	143	260	144	158	138	262
163	445	818	428	1028	461	936	417	506	636	1365
182	577	1176	579	1362	770	1673	932	1053	1326	2548
203	956	2078	762	3881	903	TL	616	699	515	TL
254	6103	TL	TL	TL	TL	TL	TL	TL	TL	TL
264	3903	6800	3422	TL	4268	TL	6453	TL	TL	TL
266	TL	TL								
275	7133	TL	6214	TL	6535	TL	TL	TL	TL	TL
295	TL	TL								
326	TL	TL								
355	TL	TL								
388	TL	TL								
410	TL	TL								
436	TL	TL								
449	TL	TL								
472	TL	TL								
482	TL	TL								
500	TL	TL								

Table 4: Run time comparison of two representations of CVaR, M3A, and M3B, for different  $\alpha$ -level/ $k$ -value for instances of size 21-500 with sample size 10

$\alpha/k$ value												
#Node	0/10				0.7/3				0.9/1			
	e-M3A	BB-M3A	e-M3B	BB-M3B	e-M3A	BB-M3A	e-M3B	BB-M3B	e-M3A	BB-M3A	e-M3B	BB-M3B
21	1	2	1	2	2	1	1	2	2	2	1	1
44	16	22	15	19	17	23	13	14	20	26	10	17
56	24	31	19	23	18	22	15	23	19	33	14	16
72	36	51	29	35	45	48	30	41	64	103	36	40
90	62	110	59	80	73	78	59	75	99	179	64	73
106	123	229	118	133	151	161	111	132	210	380	141	175
120	143	241	135	163	144	158	121	160	138	262	100	115
163	445	818	392	552	417	506	369	503	636	1365	TL	596
182	577	1550	481	738	932	1053	701	776	1326	2548	1010	1192
203	956	2078	879	1208	616	699	552	716	515	TL	452	558
254	6103	TL	TL	TL								
264	3903	6800	TL	2449	6453	TL	TL	TL	TL	TL	TL	4007
275	7133	TL	6585	TL	TL	TL	TL	TL	TL	TL	TL	TL
295	TL	TL										
326	TL	TL										
355	TL	TL										
388	TL	TL										
410	TL	TL										
436	TL	TL										
449	TL	TL										
472	TL	TL										
482	TL	TL										
500	TL	TL										

found optimal efficient set in the  $\epsilon$ -constraint method. As can be seen from Table 7, the  $\epsilon$ -constraint and the BB method do not perform well on larger instances within the time limit. However, the BB method, which bidirectionally explores the criterion space, finds more NDPs. Furthermore, the number of found NDPs and  $I_H$  values associated with the Mat method shows that it outperforms

Table 5: Run time comparison of a combination of  $\epsilon$ -constraint method (e), and the proposed matheuristic (Mat) method with M3A and M3B for different  $\alpha/k$ -values for test instances of size 21-500 with sample size of 10 scenarios.

$\alpha/k$ value													
0/10				0.7/3				0.9/1					
#Node	e-M3A	Mat-M3A	e-M3B	Mat-M3B	e-M3A	Mat-M3A	e-M3B	Mat-M3B	e-M3A	Mat-M3A	e-M3B	Mat-M3B	
21	1	0.51	1	0.42	2	0.43	1	0.43	2	0.58	1	0.46	
44	16	3	15	3	17	3	13	2	20	3	10	3	
56	24	4	19	4	18	4	15	3	19	5	14	3	
72	36	11	29	8	45	9	30	6	64	11	36	7	
90	62	18	59	16	73	23	59	19	99	21	64	14	
106	123	32	118	37	151	36	111	28	210	44	141	29	
120	143	37	135	40	144	39	121	36	138	43	100	38	
163	445	183	392	102	417	132	369	98	636	167	392	104	
182	577	212	481	140	932	178	701	128	1326	172	1010	136	
203	956	206	879	198	616	217	552	172	515	210	TL	194	
254	6103	414	TL	462	TL	589	TL	356	TL	568	TL	514	
264	3903	479	TL	652	6453	470	TL	405	TL	478	TL	445	
275	7133	686	6585	1082	TL	781	TL	711	TL	819	TL	636	
295	TL	726	TL	1068	TL	729	TL	733	TL	836	TL	775	
326	TL	893	TL	1027	TL	2407	TL	856	TL	1182	TL	914	
355	TL	1447	TL	1378	TL	1499	TL	1339	TL	1619	TL	1333	
388	TL	1611	TL	1711	TL	1835	TL	1726	TL	1931	TL	2115	
410	TL	2133	TL	2251	TL	4062	TL	2167	TL	2847	TL	1901	
436	TL	2439	TL	2413	TL	2531	TL	2340	TL	3608	TL	2220	
449	TL	2633	TL	2857	TL	2953	TL	2546	TL	2903	TL	2534	
472	TL	2955	TL	3185	TL	3167	TL	2971	TL	3194	TL	3155	
482	TL	5054	TL	4044	TL	3715	TL	3216	TL	3885	TL	3162	
500	TL	6238	TL	4442	TL	5653	TL	2955	TL	4278	TL	2358	

Table 6: Performance comparison of a combination of  $\epsilon$ -constraint method (e), and the proposed matheuristic (Mat) method with M3A and M3B for  $\alpha$ -level 0.7 and its corresponding  $k$ -value for larger number of scenarios. T[s] indicates the run time in seconds.

$\alpha/k$ value: 0.7/3													
e-M3A				Mat-M3A				e-M3B				Mat-M3B	
#Node	#Scenario	T[s]	#NDP	T[s]	#NDP	T[s]	#NDP	T[s]	#NDP	T[s]	#NDP		
21	100	161	17	27	17	56	17	5	17				
	500	6476	16	348	16	322	16	52	16				
	1000	TL	6	1668	17	TL	13	282	17				
44	100	1076	30	178	30	316	30	34	30				
	500	TL	5	1374	32	TL	19	365	32				
	1000	TL	3	TL	3	TL	7	1239	34				
56	100	2267	39	234	39	583	39	51	39				
	500	TL	3	2675	40	TL	22	776	38				
	1000	TL	3	TL	2	TL	3	1747	41				
72	100	4186	50	180	50	826	50	107	50				
	500	TL	3	TL	2	TL	15	983	51				
	1000	TL	2	TL	2	TL	2	TL	2				

the two exact methods on the large-size instances.

Performance comparison of the Mat method and the  $\epsilon$ -constraint method for small instances where the latter could find the optimal Pareto frontier is shown in Tables 8 and 9. To measure the quality, we report the hypervolume gap (gH%) and the value of  $I_\epsilon$  indicator. Analyzing the results in Table 8 confirms that the combination of Mat and M3A gives an upper bound for the Pareto frontier (as Mat is a heuristic), whereas the combination of the  $\epsilon$ -constraint method with M3B finds a lower bound for the Pareto frontier. A lower bound is obtained because the  $\epsilon$ -constraint method computes exact solutions of the approximated problem, but approximates the CVaR objective from below, as

Table 7: Hyper volume indicator values ( $I_H$ ) for the combination of  $\epsilon$ -constraint method (e), BB method and the proposed matheuristic (Mat) method with M3A and M3B models for test instances of size 21-500 with the sample size of 10 scenarios.

$\alpha/k$ value: 0.7/3																	
e-M3A			BB-M3A			Mat-M3A			e-M3B			BB-M3B			Mat-M3B		
#Node	#NDP	$I_H$	#NDP	$I_H$	#NDP	$I_H$	#NDP	$I_H$	#NDP	$I_H$	#NDP	$I_H$	#NDP	$I_H$			
21	12	3.3095	12	3.3095	12	3.3095	12	3.3098	12	3.3098	12	3.3098					
44	29	22.8869	29	22.8869	29	22.8869	29	22.8869	29	22.8869	29	22.8869					
56	35	47.6391	35	47.6391	35	47.6391	35	47.6399	35	47.6399	35	47.6399					
72	44	72.8961	44	72.8961	44	72.5908	44	72.9137	44	72.9137	44	72.9134					
90	53	146.6210	53	146.6210	53	146.5520	53	146.6260	53	146.6260	53	146.6260					
106	71	281.2760	71	281.2760	71	281.1210	71	281.3062	71	281.3055	71	281.2847					
120	77	306.7360	77	306.7360	77	306.6740	77	306.7360	77	306.7360	77	306.7360					
163	101	710.9820	101	710.9820	101	710.9820	101	710.9820	101	710.9820	101	710.9820					
182	106	746.2770	106	746.2770	106	746.2550	106	746.3030	106	746.3020	106	746.2820					
203*	115	896.4520	115	896.4520	115	896.2820	115	896.4520	115	896.4510	115	896.4340					
254	12	117.4060	120	1256.8300	135	1255.8800	8	58.7532	120	1256.8300	135	1255.6200					
275	17	212.2490	121	1722.6300	154	1723.1900	25	324.7730	127	1722.8600	155	1737.4200					
295	2	0.0000 <sup>+</sup>	89	2440.5200	155	2442.9200	2	0.0000	2	0.0000	155	2442.4200					
326	2	0.0000	35	3185.5200	176	3222.0100	2	0.0000	75	3215.0300	176	3222.7500					
355	2	0.0000	82	4236.5000	205	4250.3400	2	0.0000	148	4249.6500	205	4249.4100					
388	2	0.0000	37	4335.4900	218	4389.7100	2	0.0000	49	4352.2200	218	4416.3800					
410	2	0.0000	80	5089.8000	241	5113.6900	2	0.0000	51	4952.2200	241	5195.4300					
436	2	0.0000	112	5017.4900	246	5025.8700	28	631.8810	112	5017.4900	246	5025.8700					
449	2	0.0000	67	4838.0800	255	4866.1300	2	0.0000	63	4796.1300	255	4866.1300					
472	2	0.0000	39	5071.0500	264	5129.3900	2	0.0000	96	5124.2400	264	5129.3900					
482	3	22.9398	40	5868.9600	271	5960.6000	2	0.0000	34	5460.6000	271	5960.6000					
500	2	0.0000	35	2591.1700	181	4322.1500	2	0.0000	20	2322.1500	181	4322.1500					

Notes.  $I_H$  values are in scale of  $10^8$ .

\* marks the last instance in which the entire exact Pareto frontier is found by e and BB method.

<sup>+</sup> indicates the value of  $I_H$  where only the reference point (Nadir point) is found.

the M3B only works with a reduced number of subsets that are not necessarily worst for each NDP. Therefore, we obtain *negative* gH% values and  $I_\epsilon$  values  $\leq 1$ . Nonetheless, both methods provide high-quality approximations of Pareto frontiers as both gH%, and  $I_\epsilon$  represent a gap between the approximated sets and the reference set.

Table 8: Quality comparison using  $I_\epsilon$  and hypervolume gap (gH%) for approximated Pareto frontiers where the optimal Pareto frontier is known from solutions of solved instances using  $\epsilon$ -constraint method (e), with the sample size of 10 scenarios

$\alpha/k$ value: 0.7/3														
e-M3A (Reference set)			Mat-M3A			e-M3B								
#Node	gH%	$I_\epsilon$	gH%	$I_\epsilon$	gH%	$I_\epsilon$	gH%	$I_\epsilon$	gH%	$I_\epsilon$	gH%	$I_\epsilon$	gH%	$I_\epsilon$
21	0	1	0.00	1.00	-0.01	0.99								
44	0	1	0.00	1.00	0.00	1.00								
56	0	1	0.00	1.00	0.00	0.91								
72	0	1	0.42	1.22	-0.02	0.95								
90	0	1	0.05	1.32	0.00	0.87								
106	0	1	0.06	1.33	-0.01	0.94								
120	0	1	0.02	1.35	0.00	1.00								
163	0	1	0.00	1.00	0.00	0.96								
182	0	1	0.00	1.00	0.00	0.94								
203	0	1	0.02	1.02	0.00	0.97								

To measure the performance of the combination of the Mat method, and the M3B model, we re-evaluate the second stage of M3B model using the second objective of the M3A model, where the first stage decisions are fixed from the M3B model. In other words, in order to assess its true quality,

the solution provided by M3B is re-evaluated by using the exact second-stage objective value as obtained through M3A. As can be seen from Table 9, the e-M3B and Mat-M3B frameworks generate high-quality Pareto frontiers.

Table 9: Quality comparison using  $I_\epsilon$  and hypervolume gap (gH%) for re-evaluated approximated Pareto frontiers using e-M3B and Mat-M3B, where the optimal Pareto frontier is known from solutions of solved instances using  $\epsilon$ -constraint method (e), with the sample size of 10 scenarios

#Node	$\alpha/k$ value: 0.7/3		e-M3B		Mat-M3B	
	gH%	$I_\epsilon$	gH%	$I_\epsilon$	gH%	$I_\epsilon$
<b>21</b>	0	1	0.00	1.00	0.00	1.00
<b>44</b>	0	1	0.00	1.00	0.00	1.00
<b>56</b>	0	1	0.00	1.00	0.00	1.00
<b>72</b>	0	1	0.01	1.03	0.01	1.03
<b>90</b>	0	1	0.00	1.04	0.00	1.04
<b>106</b>	0	1	0.01	1.00	0.01	1.00
<b>120</b>	0	1	0.00	1.00	0.00	1.00
<b>163</b>	0	1	0.00	1.00	0.00	1.00
<b>182</b>	0	1	0.00	1.04	0.00	1.04
<b>203</b>	0	1	0.00	1.00	0.00	1.00

After that, we also assess the performance of re-evaluated second stage of Mat-M3B on large-size instances where the optimal Pareto frontier is not known. For this purpose, we consider a union of the Pareto frontiers ( $U$ ) obtained by e-M3A, BB-M3A, and Mat-M3A as the reference set. Table 10 shows the hypervolume gap (gH%) values. The negative value indicates that Mat-M3B with re-evaluated second stage values obtains better approximations than the union of the other methods.

Table 10: Performance of Mat-M3B on large-size instances, where the optimal Pareto-frontier is not known. The union set of Pareto frontiers obtained by e-M3A, BB-M3A, and Mat-M3B is considered as a reference set. The sample size of scenarios is 10

#Node	$\alpha/k$ value: 0.7/3	
	U (Reference set)	Mat-M3B
<b>254</b>	0.00	0.00
<b>275</b>	0.00	0.00
<b>295</b>	0.00	-0.02
<b>326</b>	0.00	-0.06
<b>355</b>	0.00	0.01
<b>388</b>	0.00	-0.10
<b>410</b>	0.00	-0.05
<b>436</b>	0.00	-0.02
<b>449</b>	0.00	-0.03
<b>472</b>	0.00	-0.08
<b>482</b>	0.00	-0.02
<b>500</b>	0.00	0.00

As an example, the Logarithmic plot of the Pareto frontier resulting from different approaches, for the instance size of 90 nodes which has the worst value of  $I_\epsilon$  is shown in Figure 2. It shows that the Mat method generates almost the same Pareto frontier as the reference set. The main differences are at the right-end of the Pareto frontier, where the location cost is high, and the uncovered demand is at the lower values.

As mentioned before, we compute the stochastic measures in order to demonstrate the effectiveness

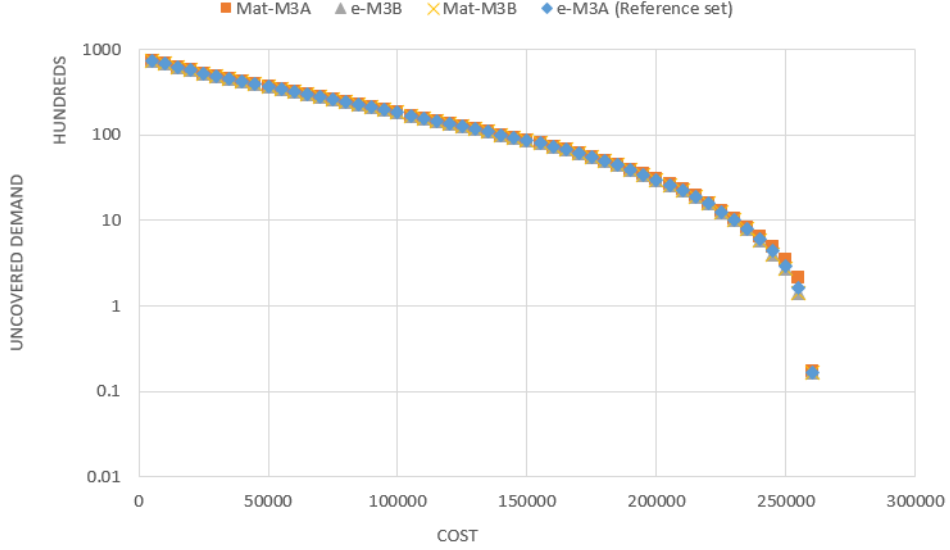


Figure 2: Logarithmic plot of Pareto frontier for the instance size 90

of incorporating the risk measure of CVaR into the model. We compute the RVPI and RVSS for different levels of  $\alpha$ . In Table 11, we report the relative values of RVPI and RVSS, which are the absolute values divided by the optimal objective value of the RRP (i.e., RVPI/RRP and RVPI/RRP). The results are the average and maximum of the computed values over all non-dominated solutions for the instance size of 21 and 44 nodes with a scenario sample size of 10. According to the results, the value of RVSS is significantly large relative to the RRP value, which indicates that it is worth to solve the risk-averse model with respect to different risk preferences. Moreover, RVPI values are also high, but they get smaller with increasing levels of  $\alpha$ .

Furthermore, we compute the RVSS values at first by fixing the value of the first-stage decisions ( $y_j$ ) based on the solutions of the deterministic average model (EA) and then, based on the risk-neutral solutions (SP). Table 12 shows the results for the instance size 21 and 44 with a scenario sample size 10. Comparing the RVSS values indicates that once the randomness has been taken into consideration, the solutions are more robust than the deterministic average model.

Table 11: Relative values of stochastic measures (RVPI/RRP, RVSS/RRP) for the instance size 21 and 44 with sample size 10

		$\alpha$ value									
		0		0.2		0.5		0.7		0.9	
#Node	#	RVSS	RVPI	RVSS	RVPI	RVSS	RVPI	RVSS	RVPI	RVSS	RVPI
		308.31	16.86	303.45	14.65	277.25	13.08	247.55	13.08	264.19	7.23
21	Avg	1969.65	70.49	1868.30	70.49	1511.80	73.86	1118.88	73.86	1237.15	38.74
	Max	7601.92	100.00	7412.21	100.00	6800.00	100.00	5570.52	100.00	3061.54	100.00
44	Avg	646.49	22.78	632.34	21.48	588.77	18.14	501.02	15.60	411.45	6.21
	Max	7601.92	100.00	7412.21	100.00	6800.00	100.00	5570.52	100.00	3061.54	100.00

Figure 3 compares the Pareto frontiers obtained by solving the RRP, the RRP with fixed first-stage solutions from the average model (REA), and the RRP with fixed first-stage solutions from the

Table 12: RVSS with fixed first-stage solutions obtained by solving the risk-neutral model (SP) compared to RVSS with fixed first-stage solutions obtained by solving the deterministic average model (EA) for the instance size 21 and 44 with sample size 10

#Node		$\alpha$ value		0		0.2		0.5		0.7		0.9	
		SP	EA	SP	EA	SP	EA	SP	EA	SP	EA	SP	EA
21	Avg	0.00	970.47	4.90	1145.94	30.77	1479.12	63.22	1903.77	88.42	2540.69		
	Max	0.00	1247.10	58.87	1483.75	240.20	1877.20	330.33	2402.66	320.00	3293.00		
44	Avg	0.00	2018.86	2.82	2373.36	35.98	3159.73	117.69	3859.85	329.62	5712.18		
	Max	0.00	2856.50	42.40	3297.00	173.60	4209.00	440.34	5160.97	868.00	7373.00		

risk-neutral model (RSP) at  $\alpha = 0.7$ . It shows that incorporating randomness in the model gives a more robust solution. Note that, the REA model obtains solutions at the left-end of the Pareto frontier that are almost as good as RRP and RSP.

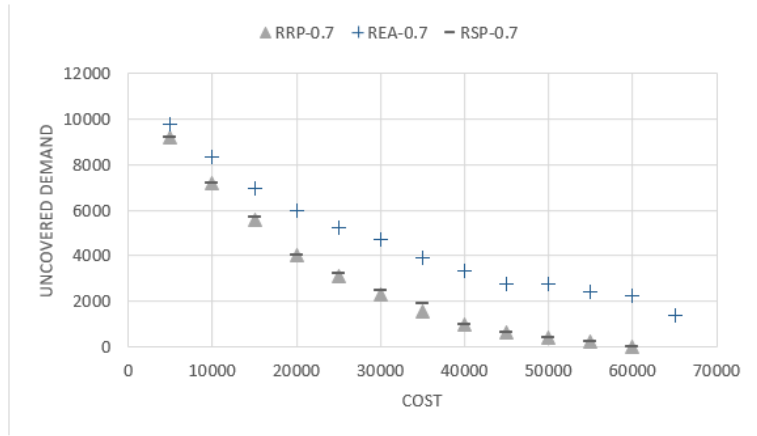


Figure 3: Pareto frontiers for instance size 21

We also compare the efficient solutions in the solution space for the average deterministic model and the CVaR model with different levels of  $\alpha$  for the instance size 21 (Figure 4). The reported solutions are associated with one point (solution 6 out of 12 Pareto solutions) along the Pareto frontier. A comparison of efficient solutions also highlights the previous finding. It shows that once the randomness in different levels of  $\alpha$  is considered, the decisions of the opened PODs ( $y_j$ ) and the allocation of demand points ( $x_{ij}$ ) are more or less similar. Whereas, these decisions in the average deterministic case are entirely different.

## 6 Conclusions

In this paper, we investigate a two-stage bi-objective location-allocation model to design a last-mile relief network. It incorporates the trade-off between a deterministic objective (minimization of location cost) and an uncertain one (minimization of uncovered demand) where demand values are uncertain.

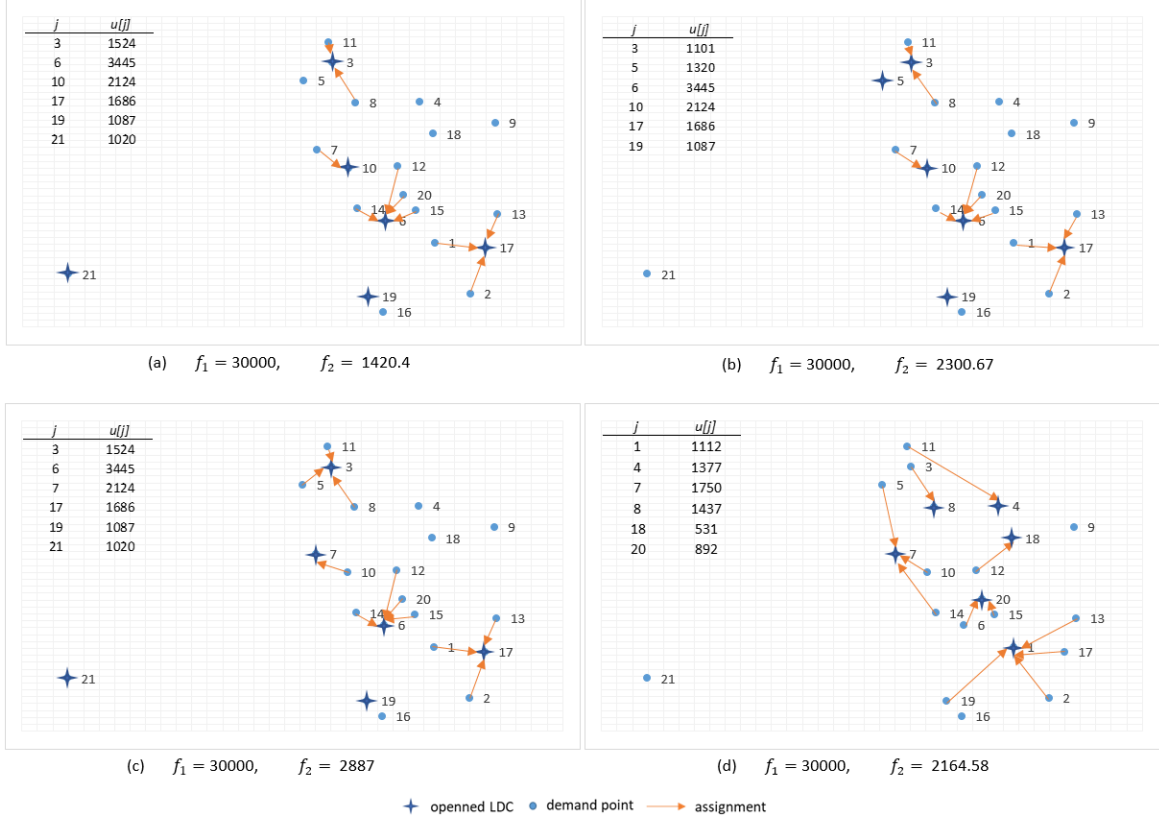


Figure 4: Comparison of the value decision variables for one the solutions of the efficient set for size 21: (a)  $\alpha = 0$ , (b)  $\alpha = 0.7$ , (c)  $\alpha = 0.9$  and (d) average deterministic case

To find an efficient and reliable methodology to address the problem, we evaluate different methods. We combined two criterion space search frameworks, the  $\epsilon$ -constraint and the balanced box methods, and three different uncertainty approaches, the widely used two-stage risk-neutral stochastic programming, two-stage adaptive robust optimization and two-stage risk-averse stochastic programming using CVaR. Two variants of linear reformulations of CVaR are taken into consideration.

We introduce a decomposition-based method to deal with the computationally challenging subset-based formulation of two-stage CVaR. Moreover, we introduce a matheuristic method in order to find high-quality approximations of the Pareto frontier for large-size instances. It is a combination of a local branching framework and the  $\epsilon$ -constraint method.

We perform a computational study and compare the results. The experiment shows that the proposed decomposition method pays off for a large number of scenarios and illustrates how the proposed matheuristic method outperforms the exact frameworks for large-size instances. Additionally, quantifying the VSS measure also shows that incorporating uncertainty into the model gives more robust results in comparison with the deterministic model. In our future research, we would like to extend the disaster relief model by considering routing constraints where there are multiple sources of uncertainty. There is also potentials for improvement of solution methods by further research on the combination of MIP and metaheuristics for bi-objective optimization.

## 7 Acknowledgment

The authors want to thank Tricoire et al. (2012) for providing us with the real-world data set of the drought case study. The Financial support from the Austrian Science Fund (FWF): P 31366-NBL is also gratefully acknowledged.

## References

Abdelaziz, F. B. (2012). Solution approaches for the multiobjective stochastic programming. *European Journal of Operational Research*, 216(1):1–16.

Altay, N. and Green III, W. G. (2006). OR/MS research in disaster operations management. *European Journal of Operational Research*, 175(1):475–493.

Balcik, B. and Beamon, B. M. (2008). Facility location in humanitarian relief. *International Journal of Logistics*, 11(2):101–121.

Ben-Tal, A., El Ghaoui, L., and Nemirovski, A. (2009). *Robust optimization*, volume 28. Princeton University Press.

Bertsimas, D., Brown, D. B., and Caramanis, C. (2011). Theory and applications of robust optimization. *SIAM review*, 53(3):464–501.

Bertsimas, D., Doan, X. V., Natarajan, K., and Teo, C.-P. (2010). Models for minimax stochastic linear optimization problems with risk aversion. *Mathematics of Operations Research*, 35(3):580–602.

Bertsimas, D., Pachamanova, D., and Sim, M. (2004). Robust linear optimization under general norms. *Operations Research Letters*, 32(6):510–516.

Birge, J. R. and Louveaux, F. (2011). *Introduction to stochastic programming*. Springer Science & Business Media.

Boland, N., Charkhgard, H., and Savelsbergh, M. (2015). A criterion space search algorithm for biobjective integer programming: The balanced box method. *INFORMS Journal on Computing*, 27(4):735–754.

Deb, K., Pratap, A., Agarwal, S., and Meyarivan, T. (2002). A fast and elitist multiobjective genetic algorithm: Nsga-ii. *IEEE transactions on evolutionary computation*, 6(2):182–197.

Ehrgott, M. (2005). *Multicriteria optimization*, volume 491. Springer Science & Business Media.

Ehrgott, M., Ide, J., and Schöbel, A. (2014). Minmax robustness for multi-objective optimization problems. *European Journal of Operational Research*, 239(1):17–31.

Fábián, C. I. (2008). Handling cvar objectives and constraints in two-stage stochastic models. *European Journal of Operational Research*, 191(3):888–911.

Fischetti, M. and Lodi, A. (2003). Local branching. *Mathematical programming*, 98(1-3):23–47.

Gralla, E., Goentzel, J., and Fine, C. (2014). Assessing trade-offs among multiple objectives for humanitarian aid delivery using expert preferences. *Production and Operations Management*, 23(6):978–989.

Grass, E. and Fischer, K. (2016). Two-stage stochastic programming in disaster management: A literature survey. *Surveys in Operations Research and Management Science*, 21(2):85–100.

Gutjahr, W. J. and Nolz, P. C. (2016). Multicriteria optimization in humanitarian aid. *European Journal of Operational Research*, 252(2):351–366.

Gutjahr, W. J. and Pichler, A. (2016). Stochastic multi-objective optimization: a survey on non-scalarizing methods. *Annals of Operations Research*, 236(2):475–499.

Haghi, M., Ghomi, S. M. T. F., and Jolai, F. (2017). Developing a robust multi-objective model for pre/post disaster times under uncertainty in demand and resource. *Journal of cleaner production*, 154:188–202.

Hoyos, M. C., Morales, R. S., and Akhavan-Tabatabaei, R. (2015). Or models with stochastic components in disaster operations management: A literature survey. *Computers & Industrial Engineering*, 82:183–197.

Ide, J. and Schöbel, A. (2016). Robustness for uncertain multi-objective optimization: a survey and analysis of different concepts. *OR spectrum*, 38(1):235–271.

Kimay, Ö. B., Saldanha-da Gama, F., and Kara, B. Y. (2019). On multi-criteria chance-constrained capacitated single-source discrete facility location problems. *Omega*, 83:107–122.

Kirkpatrick, S., Gelatt, C. D., and Vecchi, M. P. (1983). Optimization by simulated annealing. *science*, 220(4598):671–680.

Laumanns, M., Thiele, L., and Zitzler, E. (2006). An efficient, adaptive parameter variation scheme for meta-heuristics based on the epsilon-constraint method. *European Journal of Operational Research*, 169(3):932–942.

Liu, X., Küçükyavuz, S., and Noyan, N. (2017). Robust multicriteria risk-averse stochastic programming models. *Annals of Operations Research*, 259(1-2):259–294.

Mulvey, J. M., Vanderbei, R. J., and Zenios, S. A. (1995). Robust optimization of large-scale systems. *Operations research*, 43(2):264–281.

Najafi, M., Eshghi, K., and Dullaert, W. (2013). A multi-objective robust optimization model for logistics planning in the earthquake response phase. *Transportation Research Part E: Logistics and Transportation Review*, 49(1):217–249.

Noyan, N. (2012). Risk-averse two-stage stochastic programming with an application to disaster management. *Computers & Operations Research*, 39(3):541–559.

Noyan, N., Balcik, B., and Atakan, S. (2016). A stochastic optimization model for designing last mile relief networks. *Transportation Science*, 50(3):1092–1113.

Noyan, N., Merakli, M., and Küçükyavuz, S. (2019). Two-stage stochastic programming under multivariate risk constraints with an application to humanitarian relief network design. *Mathematical Programming*, pages 1–39.

Parragh, S. N., Tricoire, F., and Gutjahr, W. (2020). A branch-and-benders-cut algorithm for a bi-objective stochastic facility location problem. *arXiv preprint arXiv:2004.11248*.

Rancourt, M.-È., Cordeau, J.-F., Laporte, G., and Watkins, B. (2015). Tactical network planning for food aid distribution in kenya. *Computers & Operations Research*, 56:68–83.

Rath, S., Gendreau, M., and Gutjahr, W. J. (2016). Bi-objective stochastic programming models for determining depot locations in disaster relief operations. *International Transactions in Operational Research*, 23(6):997–1023.

Rezaei-Malek, M. and Tavakkoli-Moghaddam, R. (2014). Robust humanitarian relief logistics network planning. *Uncertain Supply Chain Management*, 2(2):73–96.

Rockafellar, R. T., Uryasev, S., et al. (2000). Optimization of conditional value-at-risk. *Journal of risk*, 2:21–42.

Steuer, R. E. and Choo, E.-U. (1983). An interactive weighted tchebycheff procedure for multiple objective programming. *Mathematical programming*, 26(3):326–344.

Tricoire, F., Graf, A., and Gutjahr, W. J. (2012). The bi-objective stochastic covering tour problem. *Computers & operations research*, 39(7):1582–1592.

Tzeng, G.-H., Cheng, H.-J., and Huang, T. D. (2007). Multi-objective optimal planning for designing relief delivery systems. *Transportation Research Part E: Logistics and Transportation Review*, 43(6):673–686.

Zhan, S.-l. and Liu, N. (2011). A multi-objective stochastic programming model for emergency logistics based on goal programming. In *Computational Sciences and Optimization (CSO), 2011 Fourth International Joint Conference on*, pages 640–644. IEEE.

Zitzler, E. and Thiele, L. (1998). Multiobjective optimization using evolutionary algorithmsa comparative case study. In *International conference on parallel problem solving from nature*, pages 292–301. Springer.

Zitzler, E., Thiele, L., Laumanns, M., Fonseca, C. M., and Da Fonseca, V. G. (2003). Performance assessment of multiobjective optimizers: An analysis and review. *IEEE Transactions on evolutionary computation*, 7(2):117–132.